 Related Commentary, page 2119

# The muscle-specific microRNA miR-206 blocks human rhabdomyosarcoma growth in xenotransplanted mice by promoting myogenic differentiation

Riccardo Taulli,[1] Francesca Bersani,[1] Valentina Foglizzo,[1] Alessandra Linari,[2] Elisa Vigna,[3] Marc Ladanyi,[4] Thomas Tuschl,[5] and Carola Ponzetto[1]

[1]Department of Anatomy, Pharmacology and Forensic Medicine, and Center for Experimental Research and Medical Studies (CeRMS), University of Torino, Torino, Italy. [2]Division of Pediatric Pathology, Ospedale Infantile Regina Margherita, Torino, Italy. [3]Division of Molecular Oncology, Institute for Cancer Research and Treatment, University of Torino, Candiolo, Italy. [4]Department of Pathology and Human Oncology & Pathogenesis Program, Memorial Sloan-Kettering Cancer Center, New York, New York, USA. [5]Howard Hughes Medical Institute, Laboratory of RNA Molecular Biology, Rockefeller University, New York, New York, USA.

**Many microRNAs (miRNAs), posttranscriptional regulators of numerous cellular processes and developmental events, are downregulated in tumors. However, their role in tumorigenesis remains largely unknown. In this work, we examined the role of the muscle-specific miRNAs miR-1 and miR-206 in human rhabdomyosarcoma (RMS), a soft tissue sarcoma thought to arise from skeletal muscle progenitors. We have shown that miR-1 was barely detectable in primary RMS of both the embryonal and alveolar subtypes and that both miR-1 and miR-206 failed to be induced in RMS cell lines upon serum deprivation. Moreover, reexpression of miR-206 in RMS cells promoted myogenic differentiation and blocked tumor growth in xenografted mice by switching the global mRNA expression profile to one that resembled mature muscle. Finally, we showed that the product of the MET proto-oncogene, the Met tyrosine-kinase receptor, which is overexpressed in RMS and has been implicated in RMS pathogenesis, was downregulated in murine satellite cells by miR-206 at the onset of normal myogenesis. Thus, failure of posttranscriptional modulation may underlie Met overexpression in RMS and other types of cancer. We propose that tissue-specific miRNAs such as miR-1 and miR-206, given their ability to modulate hundreds of transcripts and to act as nontoxic differentiating agents, may override the genomic heterogeneity of solid tumors and ultimately hold greater therapeutic potential than single gene–directed drugs.**

## Introduction

MicroRNAs (miRNAs) are a class of highly conserved, short, noncoding RNAs involved in regulating cellular and developmental events (1). miRNAs are initially transcribed as longer primary transcripts that undergo sequential processing by the RNAse III–like enzymes Drosha and Dicer (2). Mature miRNAs (21–23 nt) bind mRNAs by incomplete base pairing of their "seed sequence" to complementary sequences in the 3′ untranslated region (3′UTR) of the mRNAs (3). Although most mRNAs targeted by miRNAs are regulated by translational repression, many of them also undergo degradation (4–6).

Numerous reports have shown that miRNAs are abnormally regulated in cancer. miRNA genes are often located in genomic regions gained or lost in tumor cells (7). Some miRNAs can be functionally defined as oncogenes (8). However, global analysis of miRNA gene expression has revealed that miRNAs are generally downregulated in tumors compared with normal tissues (9). Furthermore, inhibiting miRNA processing enhances tumorigenesis (10), suggesting that miRNAs act mainly as oncosuppressors. The list of miRNAs that interfere with the tumorigenic properties of various cancer cell lines is rapidly expanding, and in some cases, there is also in vivo evidence that miRNAs can function as tumor suppressors (11–14).

Many miRNAs are expressed in a tissue-specific manner, implying important functions in differentiation (15–18). Among them, the so called myomiRs (reviewed in ref. 19) represent a well-defined family, consisting of 3 bicistronic pairs (miR-1-1/miR-133a-2, miR-1-2/miR-133a-1, miR-206/miR-133b). miR-1-1 and miR-1-2 are identical, and miR-206 differs from them only for 3 nucleotides, all outside the seed sequence. miR-133a-2, miR-133a-1, and miR-133b are identical as well, except for 1 nucleotide at the 3′ end of miR-133b. Thus, each of these miRNA trios can target the same mRNAs. The myomiRs are primarily involved in heart and skeletal muscle development. miR-206 is the only one specific to skeletal muscle. Its expression is higher than that of miR-1 during development and perinatally (20, 21) but in adult muscle is much lower than that of miR-1 (17).

While it has been proposed that miR-133 enhances myoblast proliferation (22), there is strong evidence that miR-1 and miR-206 promote muscle differentiation (23). Following transfection of physiological levels of either miR-1 or miR-206, C2C12 myoblasts undergo myogenic differentiation, without need for

**Authorship note:** Riccardo Taulli and Francesca Bersani contributed equally to this work.

**Conflict of interest:** The authors have declared that no conflict of interest exists.

**Nonstandard abbreviations used:** ARMS, alveolar RMS; AS, antisense; ERMS, embryonal RMS; GBM, glioblastoma multiforme; hMB, human myoblast; LNA, locked nucleic acid; MHC, myosin heavy chain; miRNA, microRNA; MyoD, myogenic differentiation factor 1; RMS, rhabdomyosarcoma; 3′UTR, 3′ untranslated region.

**Citation for this article:** *J. Clin. Invest.* **119**:2366–2378 (2009). doi:10.1172/JCI38075.

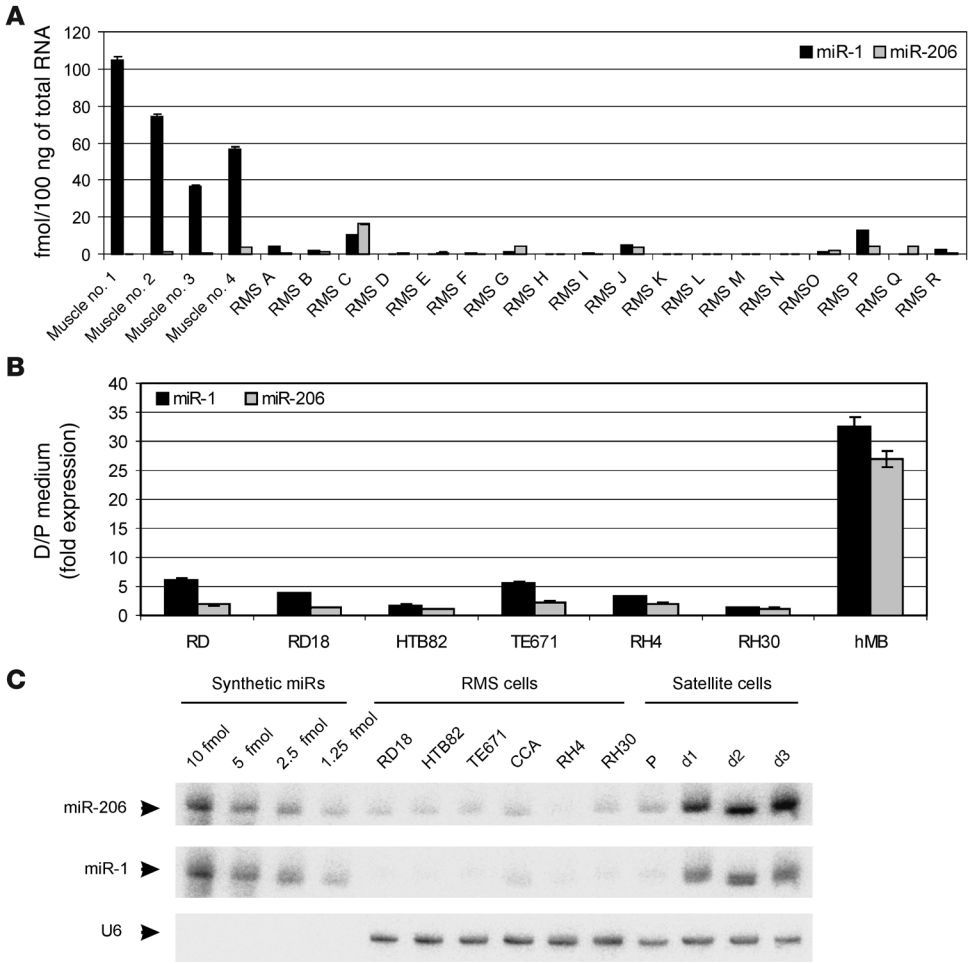


**Figure 1**
miR-1 is poorly expressed in primary tumors, and RMS cells switched to differentiating conditions fail to induce miR-1/miR-206. (**A**) Quantitative real-time PCR analysis of mature miR-1 and miR-206 in primary human RMS (A–R) and control muscles (no. 1–4). Mean values (± SD) are from 3 replicates. (**B**) Increase of expression of mature miR-1/miR-206 in RMS cells and control hMBs in differentiation medium (D, medium with low levels of serum) relative to proliferation medium (P, medium with high levels of serum), measured by real-time PCR. Mean values (± SD) are from 3 independent experiments. (**C**) Northern blot with miR-206– and miR-1–specific probes on total RNA (5 μg/lane) obtained from the indicated RMS cells grown for 3 days in differentiation medium and from proliferating and differentiating murine satellite cells. Increasing amounts of synthetic miRNAs were used as standards for quantification.

serum depletion, suggesting that these miRNAs are particularly important for the induction of cell quiescence (23). Furthermore, forced expression of miR-1 in HeLa cells causes, in the short term, downregulation of hundreds of genes, most of which are expressed at low levels in muscle relative to other tissues (4). Analogous results were obtained by ectopically expressing in Hela cells a neural miRNA (miR-124), indicating that tissue or cell-type specific miRNAs, such as miR-1, miR-206, and miR-124, tend to shift the mRNA expression profile toward that of the tissue in which they are enriched.

Rhabdomyosarcomas (RMSs), the most common soft tissue sarcomas in pediatric patients and young adults, coexpress markers of proliferation and myogenic differentiation (24). The current histological classification of RMS defines 2 major subtypes (embryonal RMS [ERMS] and alveolar RMS [ARMS]), differing in body location, occurrence, mean patient age, and prognosis. The alveolar subtype is less common but has a worse outcome, being frequently metastatic at diagnosis. While most ARMSs carry the pathogenetic translocation PAX3/7-FKHR (25, 26), ERMSs do not carry a distinct genetic lesion and generally follow a more favorable course. The expression profiles of ARMSs and ERMSs differ widely (27), but cell lines established from both types of tumor, as well as primary tumors, consistently express rather high levels of the Met receptor (28), a potential target of miR-1 and miR-206.

We have shown in previous work that Met is necessary for the survival and proliferation of cell lines derived from both RMS subtypes, in culture and in vivo (29). In this work, we asked whether, in RMS, sustained Met expression could derive from lack of posttranscriptional downregulation by myomiRs and thus whether they could have therapeutic value. We found that in RMS cells miR-1 and miR-206 fail to be induced following growth factor withdrawal. On the other hand, in normal myoblasts, at the onset of myogenesis, Met is indeed posttranscriptionally downregulated. We provided evidence for Met being a primary target of miR-206, and we showed that forced expression of miR-206 caused a major switch in the global expression profile toward mature muscle, rescued differentiation of both ERMS and ARMS, and blocked tumor growth.

## Results

*miR-1 expression is low in primary RMS, and RMS cells fail to induce miR-1 and miR-206 upon being switched to differentiation medium.* We first determined the level of expression of miR-1 and miR-206 in 4 control muscles and in a panel of primary RMSs, including 10 ERMSs and 8 ARMSs. As expected, in control muscle, the absolute level of miR-1 was, on the average, over 60 times that of miR-206. In line with 2 previous reports (30, 31), we found that in RMS tumors, expression of miR-1 was absent or of the same order as miR-206 (Figure 1A).

Considering that miR-1 and miR-206 are normally strongly upregulated at the onset of myogenesis (23), we next verified wheth-

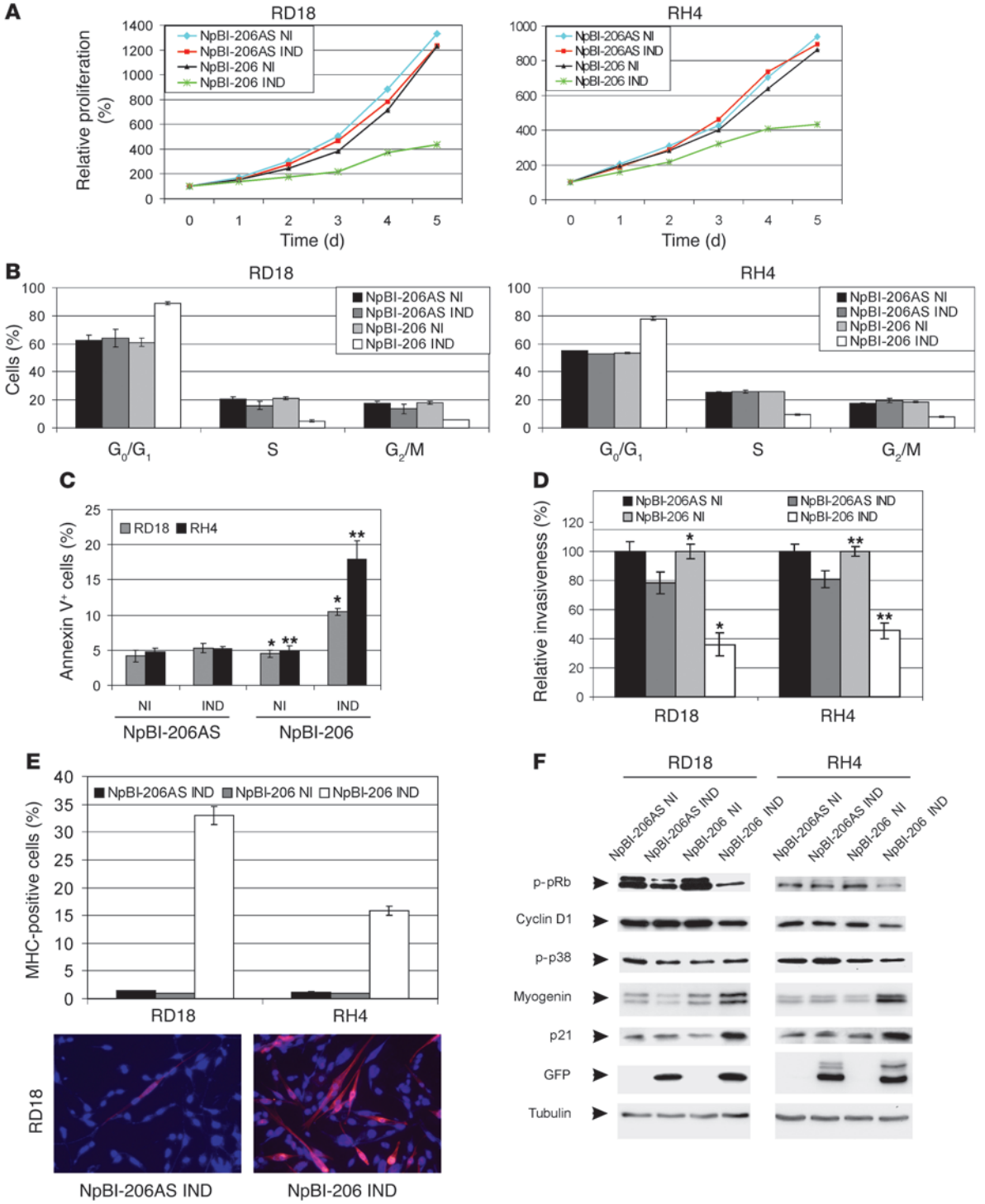
A
RD18
RH4
Relative proliferation (%)
Time (d)
NpBI-206AS NI
NpBI-206AS IND
NpBI-206 NI
NpBI-206 IND
B
RD18
RH4
Cells (%)
G0/G1
S
G2/M
C
Annexin V+ cells (%)
RD18
RH4
NI
IND
NpBI-206AS
NpBI-206
D
Relative invasiveness (%)
E
MHC-positive cells (%)
RD18
RH4
NpBI-206AS IND
NpBI-206 IND
F
p-pRb
Cyclin D1
p-p38
Myogenin
p21
GFP
Tubulin

**Figure 2**
Conditional expression of miR-206 in RMS cells causes reduction of cell proliferation and cell cycle arrest in the $G_0/G_1$ phase, increases apoptosis, decreases invasiveness, and enhances myogenic differentiation. Cells were infected with either the control or the miR-206–expressing vector (NpBI-206AS and NpBI-206, respectively; see Methods) (Tet-off system) and treated (noninduced, NI) or not (induced, IND) with doxycycline (Dox). (**A**) Proliferation was evaluated for a period of 5 days. The number of cells at day 0 was set at 100%. (**B**) Cell-cycle distribution of RMS cells in presence/absence of doxycycline was measured by propidium iodide staining and FACS analysis. (**C**) Apoptosis was measured by Annexin V–allophycocyanin staining and FACS analysis. (**D**) Invasiveness was evaluated 72 hours after seeding RMS cells in matrigel-coated transwell chambers. (**E**) MHC expression in RMS cells upon miR-206 induction in medium with high levels of serum compared with controls. Values represent counts of 6 fields for each group normalized against the number of DAPI-positive cells in the same fields (top). Representative immunofluorescence images of induced RD18 cells carrying the NpBI-206AS and the NpBI-206 vector, respectively (bottom). Blue staining was performed with DAPI; red staining was performed with MHC. Original magnification, ×20. (**F**) Western blot of phospho-pRb, cyclin D1, phospho-p38, myogenin, p21, GFP, and tubulin on noninduced and induced RD18 and RH4 cells (30 μg/lane). All mean values (± SD) are from 3 independent experiments (**A**–**E**). $^*P < 0.05$; $^{**}P < 0.05$ (Student's *t* test).

er in ERMS and ARMS cell lines their level of expression changed upon switching from proliferating to differentiating conditions. We found that induction of these myomiRs was reduced or absent in RMS cells with respect to primary human myoblasts (hMBs) (Figure 1B). This result was confirmed by Northern blot. In all RMS cells switched to differentiation medium, the levels of miR-1 and miR-206 remained very low, similar to that of proliferating murine myoblasts (Figure 1C).

*Reexpression of miR-1 and miR-206 in ERMS and ARMS cell lines interferes with the transformed phenotype and promotes myogenic differentiation.* To verify whether the inability to upregulate miR-1 and miR-206 was responsible for blocked differentiation typical of RMS (32), we reintroduced them in RMS cells. To this end, we produced lentiviral vectors constitutively expressing pre–miR-1 and –miR-206, along with GFP. We found that reexpression of miR-1 and miR-206 caused an approximately 50% reduction in soft agar colony formation in RMS cell lines (Supplemental Figure 1, A and C; supplemental material available online with this article; doi:10.1172/JCI38075DS1). Observation at the fluorescence microscope revealed that the surviving colonies were composed of cells with either low or no GFP expression, indicating that only cells with low levels of miR-1/miR-206 were able to grow in an anchorage-independent manner.

Furthermore, a few days after miR-1 and miR-206 transduction, a substantial number of RMS cells underwent myogenic differentiation, as indicated by their positivity for myosin heavy chain (MHC), even when grown in proliferation medium (Supplemental Figure 1, B and D). However, keeping the cells in culture for a longer time resulted in positive selection of those with low or no GFP, which ultimately outnumbered the differentiated ones (data not shown).

Thus, especially in order to test the effects of the miRNAs in vivo, we set up an inducible lentiviral system, which allowed selection of high expressers by sorting the cells, following a brief pulse of induction, on the basis of their green fluorescence. Since miR-206 was expressed more efficiently than miR-1 and the 2 miRs are virtually identical, we chose to continue our studies using the inducible miR-206–expressing vector.

Bringing expression of miR-206 to a level comparable to that of differentiating murine satellite cells (Supplemental Figure 2) caused a strong reduction in the proliferation of both ERMS and ARMS cells (Figure 2A). Accordingly, cell-cycle analysis (done 72 hours after miR-206 induction) showed an accumulation in the $G_0/G_1$ phase and a concomitant reduction in the S and $G_2/M$ phases of the cell cycle (Figure 2B). miR-206 also promoted apoptosis, as shown by Annexin V staining (Figure 2C) and decreased Matrigel invasiveness (Figure 2D). Six days after miR-206 induction, the number of MHC-positive cells in ERMS and ARMS cultures increased about 30 and 15 fold, respectively (Figure 2E, top panel). MHC-positive cells were often elongated and multinucleated (Figure 2E, bottom panels), indicating terminal myogenic differentiation. To explore the effect of miR-206 expression on key molecules of the myogenic lineage, we analyzed by Western blot proteins involved in cell proliferation and differentiation. While phosphorylation of p38 MAPK was not affected, miR-206 caused downregulation of cyclin D1 and phospho–retinoblastoma protein (phospho-pRb) and upregulation of p21 and myogenin (Figure 2F). These changes are consistent with exit from the cell cycle and activation of the myogenic program.

*Induction of miR-206 expression promotes RMS differentiation by modulating more than 700 genes.* To substantiate the above conclusion at the level of global gene expression, we determined the long-term changes in the mRNA profile of RD18 cells before and after miR-206 induction using microarrays (Figure 3A). As a control, we used RD18 cells transduced with the inducible vector expressing miR-206 in antisense (AS). We focused on the 734 genes that were most significantly ($P < 0.05$) induced (278 genes, violet cluster in the vertical axis of the dendrogram) or repressed (456 genes, green cluster in the vertical axis of the dendrogram) after doxycycline treatment. Unsupervised hierarchical clustering (including also the data from 3 normal skeletal muscles biopsies) generated a dendrogram with 2 major branches, one of which contained the noninduced (NI) miR-206 and both the NI and induced (IND) miR-206AS RD18 cells, while the second one grouped both normal muscles and RD18 cells in which miR-206 expression was induced for 3 and 6 days, respectively. The results of this experiment indicated that, on the whole, expression of miR-206 indeed shifted the global gene expression profile of RMS cells toward that of differentiated muscle, with the exception of 2 minor clusters of genes (blue and yellow in the vertical axis of the dendrogram), which after induction were differentially expressed with respect to mature muscle.

The extent of the RMS-to-muscle shift in gene expression depended on the length of miR-206 induction. In fact, the Pearson correlation between RD18 cells and muscle increased from 0.01 in NI cells (data not shown) to 0.55 and 0.68 in cells treated with doxycycline for 3 and 6 days, respectively (Figure 3B). To characterize the genes that were modulated by miR-206 in RD18 cells, we assigned them to functional categories. The more significantly upregulated genes ($P < 0.05$) were enriched for muscle-related functions, while the more significantly downregulated genes included those involved in the control of cell cycle, metabolism, and DNA repair (Table 1 and Supplemental Table 1). Using the EIMMo miRNA target prediction server (http://www.mirz.unibas.ch/ElMMo2/), we found among the downregulated genes a number of predicted miR-206 targets, including Met (19). A list is provided in Supplemental Table 2. In sum, our microarray analysis provided strong evidence for the induction of muscle differentiation upon expression of miR-206 in RMS cells.

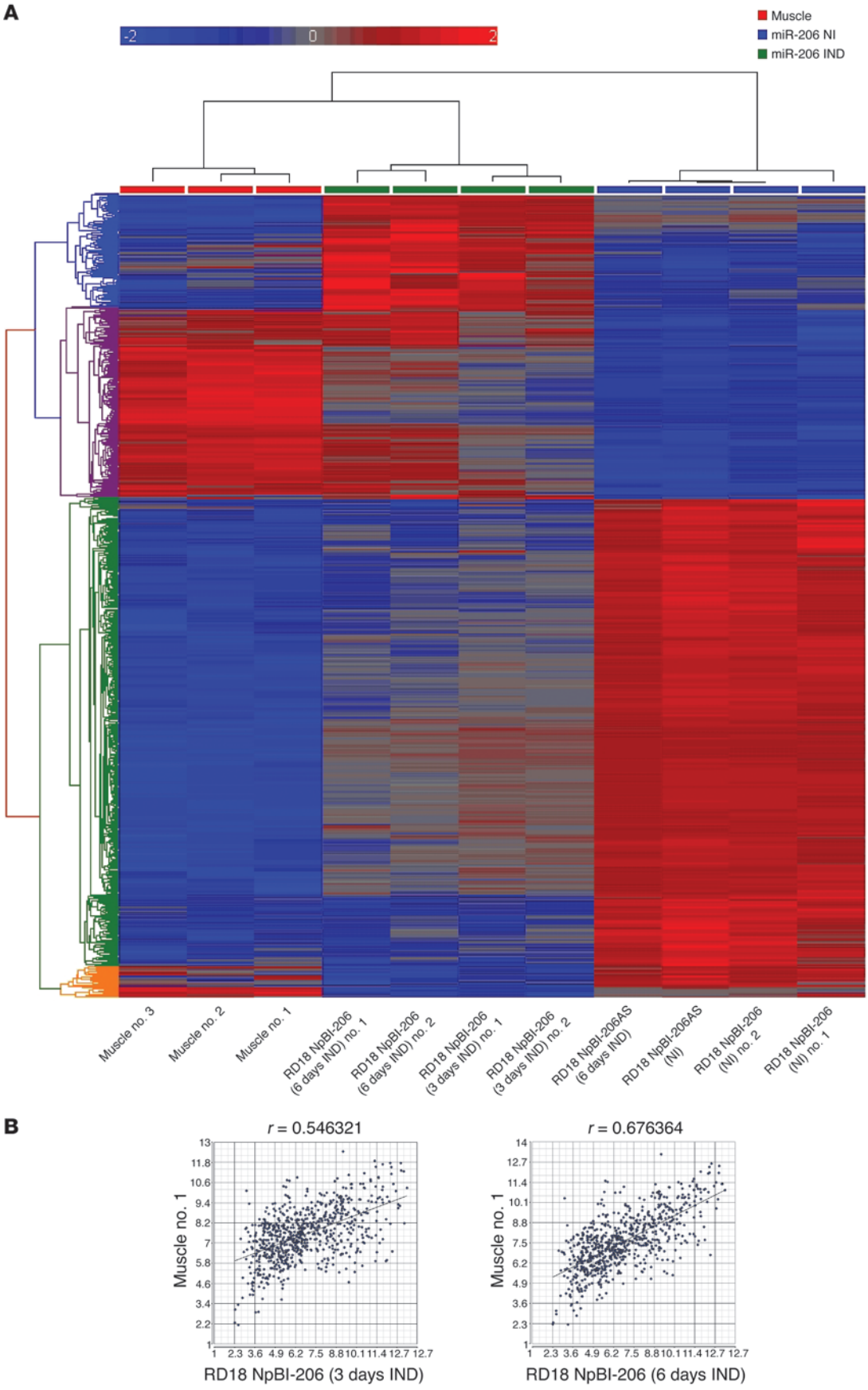
A
-2
0
2
Muscle
miR-206 NI
miR-206 IND
Muscle no. 3
Muscle no. 2
Muscle no. 1
RD18 NpBI-206 (6 days IND) no. 1
RD18 NpBI-206 (6 days IND) no. 2
RD18 NpBI-206 (3 days IND) no. 1
RD18 NpBI-206 (3 days IND) no. 2
RD18 NpBI-206AS (6 days IND)
RD18 NpBI-206AS (NI)
RD18 NpBI-206 (NI) no. 2
RD18 NpBI-206 (NI) no. 1
B
r = 0.546321
Muscle no. 1
RD18 NpBI-206 (3 days IND)
r = 0.676364
Muscle no. 1
RD18 NpBI-206 (6 days IND)

**Figure 3**
Induction of miR-206 shifts the global gene expression profile of RMS cells toward that of muscle. (**A**) Unsupervised hierarchical clustering of muscles and NpBI-206 and NpBI-206AS RD18 cells prior to (miR-206 noninduced) and after (miR-206 induced) doxycycline administration (Tet-on system) for the indicated times. Only genes showing a fold change of more than 2 and a *t* test *P* value of less than 0.05 were included in the analysis. Red indicates increased expression; blue indicates reduced expression. (**B**) Pearson correlation of miR-206–expressing RD18 cells (3 and 6 days after induction) compared to normal muscle number 1.

*Induction of miR-206 expression blocks the growth of RMS xenografts in vivo by promoting myogenic differentiation*. These results suggested that by tilting the balance of RMS cells toward differentiation, miR-206 could act as a tumor suppressor in vivo. To assess whether induction of miR-206 could prevent tumor growth, lentiviral-transduced ERMS and ARMS cells were injected into immunocompromised mice, kept either in inducing or noninducing conditions (see legend of Figure 4). Both ERMS and ARMS cells, after a slightly different lag time, formed rapidly growing tumors in animals in which miR-206 was not induced. Continuous miR-206 expression essentially suppressed the growth of both types of tumor (Figure 4, A and B). To assess whether miR-206 could have therapeutic potential for RMS treatment, we induced it in vivo when the tumors reached approximately 0.4 $cm^3$ in volume and when the tumors became much larger. While no effect was observed upon induction of the control AS construct, in all cases, miR-206 expression efficiently blocked tumor growth (Figure 4, C–F). Histological analysis revealed a striking change in the morphology of the tumor cells (data not shown), indicating a massive switch to the differentiated phenotype. The switch was confirmed by immunohistochemistry with Ki67- and MHC-specific antibodies, which showed that most cells were no longer replicating (Ki67 negative) and appeared to be terminally differentiated (MHC positive) (Figure 4, G and H). The presence of miR-206 in the tumor tissue after induction was verified by real-time PCR (Figure 4I).

*Met is posttranscriptionally downregulated by miR-206 during myogenic differentiation and is silenced following miR-206 expression in RMS cells*. There are several potential targets of miR-1 and miR-206 (19), which could contribute to the malignant phenotype of RMS cells. We focused on Met, a tyrosine kinase receptor overexpressed in primary RMS tumors and cell lines, which has been implicated in RMS pathogenesis (28, 29). Physiologically, Met is rapidly downregulated at the onset of myogenic differentiation (33). To assess whether this process involves posttranscriptional mechanisms, we used murine satellite cells. When grown in medium with high levels of serum, satellite cells actively proliferate. However, within 3 to 4 days of switching to medium with low levels of serum, they differentiate into myotubes (Figure 5A, top panel). Both miR-1 and miR-206 increased after the switch (Figure 5A, bottom panel). Myogenin (a transcription factor that directly induces muscle-specific genes) and MHC (one of its targets and a marker of terminal differentiation) were rapidly upregulated. Conversely, the Met protein was almost completely downregulated, starting at day 1 after the switch, with total depletion by day 3 (Figure 5B). Interestingly, downregulation of the *Met* transcript followed a much slower kinetic. In fact, at day 4 of differentiation, *Met* mRNA was still present at 40% of the original level (Figure 5C). These results suggest that in myogenic cells, at the onset of differentiation, Met is posttranscriptionally downregulated.

The *Met* transcript has 2 conserved binding sites for miR-1/miR-206 in its 3′UTR. To verify whether endogenous miR-1/miR-206 could be responsible for the rapid downregulation of Met observed upon switching to medium with low levels of serum, we transfected satellite cells with a sensor vector expressing GFP linked to the Met 3′UTR. Upon switching to medium with low levels of serum, when expression of endogenous miR-1/miR-206 was induced (Figure 5A), we observed a decrease of both endogenous Met and of the transfected GFP protein (Figure 6A). This effect was specifically abrogated by the locked nucleic acid (LNA) complementary to miR-206, which also impaired morphological differentiation of the cells (data not shown). To verify whether the Met 3′UTR was indeed a miR-206 target, we cotransfected RD18 cells with a GFP sensor, including only the 2 miR-1/miR-206 recognition motifs found in the Met 3′UTR, either wild type or point mutated. FACS analysis done 48 hours after transfection revealed a strong decrease of green fluorescence in the samples cotransfected with miR-206 and the wild-type sensor. There was no downregulation in cells cotransfected with the point-mutated sensor (Figure 6B).

Finally, we verified whether the level of miR-206 expression obtained with the inducible lentiviral vector was sufficient to suppress the Met protein in ERMS and ARMS. In both cases, induction of miR-206 caused a marked reduction of the Met protein levels in cultured cells in concomitance to the enhancement of differentiation (Figure 6C). An analogous decrease of Met protein level was detected in miR-206–expressing xenografts (Figure 6D). On the other hand, expressing the constitutively active form of the receptor (Tpr-Met [34], devoid of the 3′UTR) together with

**Table 1**
Top 11 enriched functional categories of genes modulated by miR-206 induction in RD18 cells (corrected *P* value of less than 0.05)

| Category | *P* value |
|---|---|
| **Upregulated genes** | |
| Muscle system process | $5.80 \times 10^{-13}$ |
| Muscle contraction | $5.80 \times 10^{-13}$ |
| Muscle development | $1.00 \times 10^{-5}$ |
| Regulation of muscle contraction | $3.00 \times 10^{-3}$ |
| System process | $2.40 \times 10^{-2}$ |
| System development | $2.80 \times 10^{-2}$ |
| Striated muscle contraction | $3.10 \times 10^{-2}$ |
| Anatomical structure development | $3.10 \times 10^{-2}$ |
| Cellular component organization and biogenesis | $4.30 \times 10^{-2}$ |
| Organ development | $3.90 \times 10^{-2}$ |
| Multicellular organismal process | $3.60 \times 10^{-2}$ |
| **Downregulated genes** | |
| Cell cycle | $1.30 \times 10^{-65}$ |
| Cell-cycle process | $7.10 \times 10^{-58}$ |
| M phase | $8.80 \times 10^{-58}$ |
| Mitosis | $2.40 \times 10^{-57}$ |
| M phase of mitotic cell cycle | $3.70 \times 10^{-57}$ |
| Cell-cycle phase | $3.60 \times 10^{-57}$ |
| Mitotic cell cycle | $5.40 \times 10^{-56}$ |
| Cell division | $8.10 \times 10^{-54}$ |
| DNA metabolic process | $1.20 \times 10^{-45}$ |
| DNA replication | $8.50 \times 10^{-32}$ |
| Organelle organization and biogenesis | $2.40 \times 10^{-24}$ |

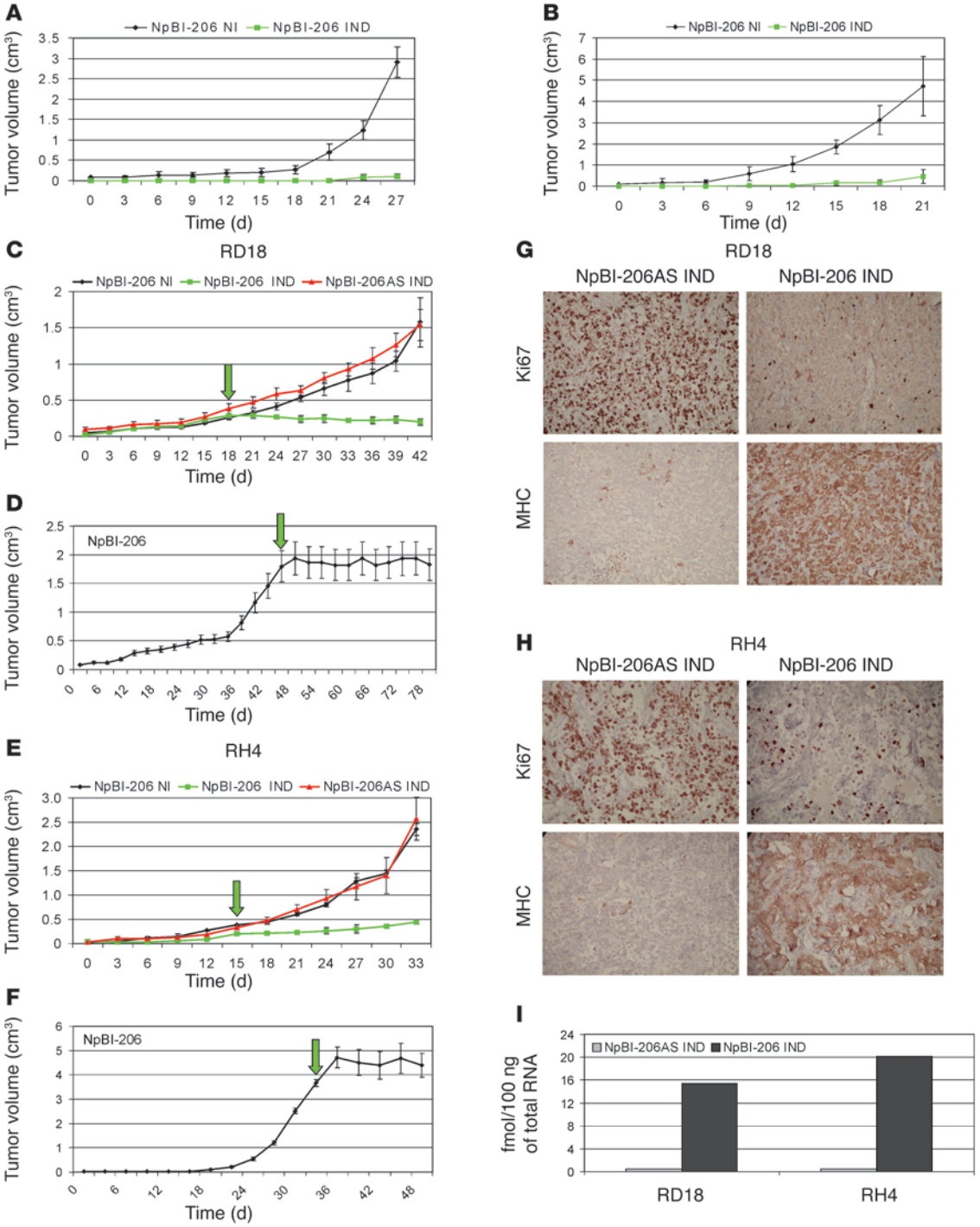


**Figure 4**

miR-206 arrests growth of RMS xenografts by promoting myogenic differentiation. (**A** and **B**) Continuous expression of pre–miR-206 (green lines) prevents growth of (**A**) embryonal (RD18) and (**B**) alveolar (RH4) RMS xenografts. In the Tet-off system, half of the mice ($n$ = 5) were administered drinking water containing 1 mg/ml doxycycline, starting at the time of injection (noninduced), while the rest received water alone (induced). (**C** and **E**) Inducible expression of pre–miR-206 arrests growth of (**C**) RD18 and (**E**) RH4 xenografts. In the Tet-on system, 5 of 10 mice bearing RMS tumors were given drinking water containing 1 mg/ml of doxycycline, starting on the day indicated by the arrow (green lines, pre–miR-206 induced; black lines, pre–miR-206 noninduced; red lines, AS pre–miR-206 induced [$n$ = 5]). (**D** and **F**) miR-206 induction (Tet-on) in advanced RD18 ($n$ = 3) and RH4 ($n$ = 3) tumors is sufficient to block their growth. Doxycycline treatment started on the day indicated by the green arrow. Tumor growth was measured every 3 days, starting when the tumors became palpable (day 0). Bars indicate SEM (**A**–**F**). (**G** and **H**) Immunohistochemical analysis of sections of tumors harvested from doxycycline-treated animals. Ki67-specific antibody was used as a marker for proliferating cells; MHC-specific antibody was used as a marker for differentiated cells. Original magnification, ×20. (**I**) Representative quantitative real-time PCR analysis of mature miR-206 in RMS xenografts recovered from doxycycline-treated (1 week) and untreated animals.

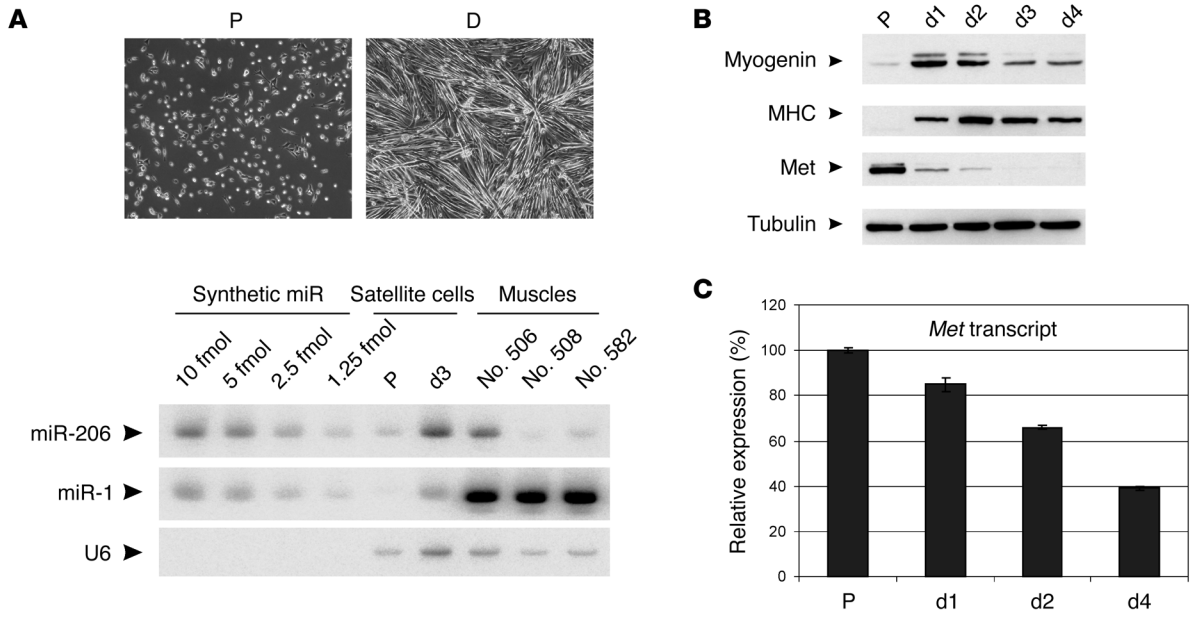


**Figure 5**

Met is posttranscriptionally downregulated during myogenic differentiation. (**A**) Murine satellite cells grown in proliferation medium (top left panel), differentiate into myotubes when switched to medium with low levels of serum (top right panel). Original magnification, ×20. Representative Northern blot of total RNA (5 μg/lane) from satellite cells (proliferating and at 3 days of differentiation) and adult murine muscles (mouse number 506, 508, and 582), probed for miR-1/miR-206 expression. U6 was used as loading control. Increasing amounts of synthetic miRNAs were used as standards for quantification. (**B**) Western blot of extracts of satellite cells, either proliferating or at different stages of differentiation (day 1–4), probed for myogenin, MHC, Met, and tubulin as a control. Thirty micrograms of protein extracts were loaded in each lane. (**C**) Real-time PCR on Met on the same cells. The level of *Met* transcript in proliferating cells was set at 100%. Mean values (± SD) are from 3 independent experiments.

miR-206, in RD18 cells, significantly increased proliferation and invasiveness (Supplemental Figure 3, A and B), while decreasing apoptosis and MHC-positive cells (Supplemental Figure 3, C and D). In vivo, the effect of Tpr-Met on the rescue of tumor growth was even more evident, probably due to the proliferative advantage of cells that express high levels of Tpr-Met (Supplemental Figure 3E). These results indicate that Met is an essential target for the therapeutic effect of miR-1/miR-206 in RMS.

## Discussion

In this work, we showed that miR-1, which promotes myoblast differentiation, is markedly and reproducibly underrepresented in primary RMS and in RMS cell lines, relative to nonneoplastic muscle tissue. For its essentially identical paralog, miR-206, which in mature muscle is roughly 2 orders of magnitude lower than miR-1 and can also vary, depending on the relative abundance of slow- versus fast-twitch fibers (35), the downregulation in tumors relative to normal muscle is less clear cut. However, it is important to note that, following growth factor deprivation, both miRNAs failed to be induced in RMS cell lines.

In the attempt of identifying a molecular lesion responsible for this defect, we searched for mutations in the predicted myogenic differentiation factor 1–binding (MyoD-binding) and myogenin-binding sites, located upstream of the *Mir1/MiR206* genes (36). In parallel, we also looked for possible mutations in the precursors that could compromise their maturation. However, we did not find any significant change in the DNA sequence of RMS cell lines compared to normal muscle controls. An alternative possibility was methylation/deacetylation (14, 37), but treatment with either the demethylating agent 5Aza-2-deoxycytidine or the histone deacetylase inhibitor Trichostatin A did not enhance miR-1/miR-206 expression in RMS cells. The failure to upregulate transcription of the myomiRs may simply be due to the fact that in RMS, MyoD seems to be nonfunctional, despite its ability to associate with coactivators and to bind to DNA (38).

Re-adjusting miR-206 expression in RMS cells at a level comparable to that of differentiating satellite cells suppressed many aspects of the transformed phenotype. However, the most striking effect was the induction of myogenic differentiation, which occurred even in the presence of growth factors. Thus, miR-206 was sufficient to force the neoplastic cells into resuming and completing the myogenic program. This occurred without changes in the phosphorylation of p38. Once activated, p38 promotes the sequential activation of muscle regulatory factors and their transcriptional coactivators, including chromatin remodelling enzymes (reviewed in ref. 39). Sustained activation of p38 has been proposed as the missing factor required for rescuing MyoD activity in RMS cells. In fact, forced expression of the constitutively active upstream kinase MKK6-EE in RD and RH30 cells in culture was sufficient to increase morphological and biochemical differentiation (40). Since miR-206 induced differentiation without changes in p38 phosphorylation, this miRNA may bypass the need for p38 activation by acting downstream of it or through parallel pathways.

Gene expression analysis via microarray revealed that miR-206 expression in RMS cells caused a major switch toward a muscle-like profile, as indicated by the fact that among the more than 270 genes found to be upregulated, many were muscle-specific, such as

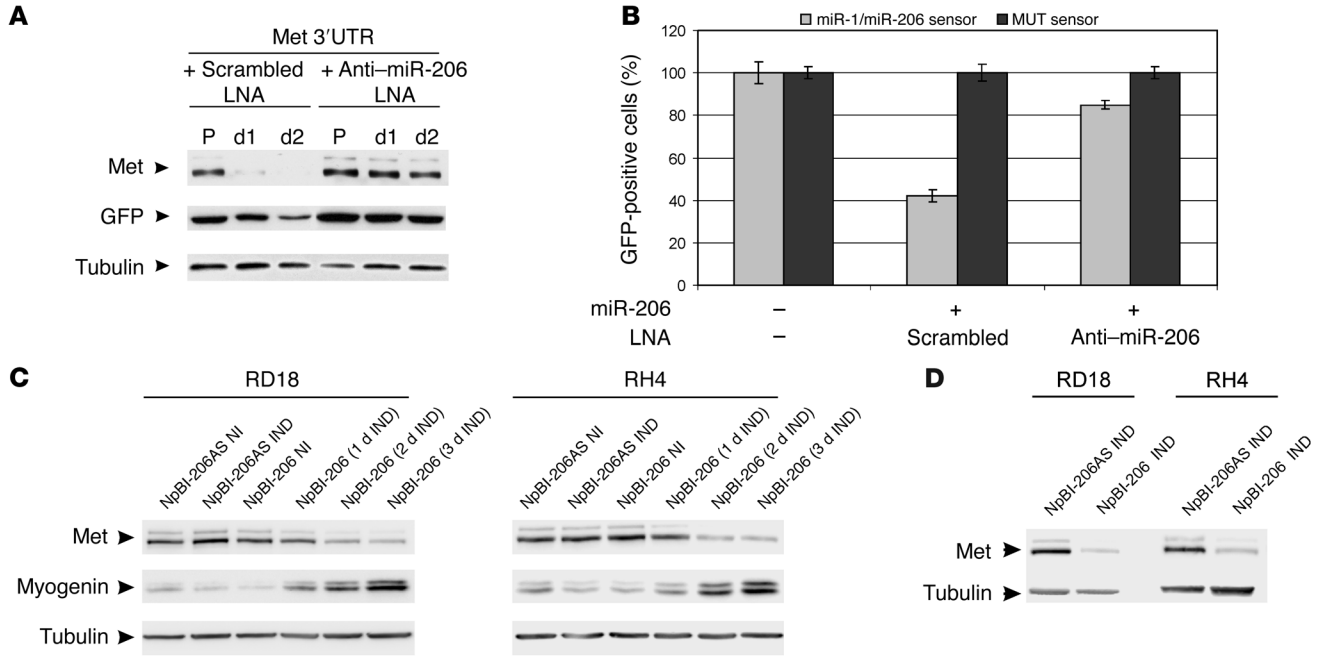


**Figure 6**

Met is posttranscriptionally downregulated by miR-206 by direct targeting of its 3′UTR. (**A**) Western blot of Met, GFP, and tubulin on protein extracts (30 μg/lane) of murine satellite cells transfected with the Met 3′UTR reporter construct along with a scrambled or miR-206–directed LNA (400 nM) and then switched to differentiation medium for 1 to 2 days. The difference in the kinetics of Met and EGFP downmodulation is most likely due to the long half-life of this form of GFP (stabilized). (**B**) GFP quantification by FACS analysis on RD18 cells transfected with either a miR-1/miR-206 sensor vector (see Methods) or a point-mutated (MUT) sensor vector along with a scrambled or miR-206–directed LNA (400 nM). The GFP level of control cells was set at 100%. Mean values (± SD) are from 3 independent experiments. (**C** and **D**) Western blot on protein extracts of noninduced and induced RD18 and RH4 (**C**) cells probed for Met, myogenin, and tubulin and (**D**) RMS xenografts probed for Met and tubulin. Thirty micrograms of protein extracts were loaded in each lane.

titin, muscle creatine kinase, myosin light chain, troponin C, myomesin 2, and tropomyosin 2. Of the more than 450 downregulated genes many were involved in the cell cycle and DNA metabolism and repair. Conversely, the 2 minor subsets of genes, whose level of expression was more similar to normal muscle in the uninduced rather than in the induced RD18 cells, did not show any significant enrichment for specific functional categories. It is possible that a transient inverse modulation of these genes might be necessary for the conversion from proliferating to differentiated cells. The time dependency of the switch indicates that most of the observed effects of miR-206 were indirect, but among the downregulated mRNAs, there were also validated (Pola1 [23], PTBP1 [41]) and predicted (CDK2) direct targets of miR-206. This finding is in line with the emerging concept that in some cases a major component of miRNA-mediated repression is mRNA destabilization (5, 6).

We were particularly interested in the role of miR-1/miR-206 on another recently validated target, the Met receptor (37, 14), which is activated by overexpression in many cancers, including RMS (28, 29). We found that in normal myogenic cells, at the onset of myogenesis, Met is rapidly downregulated by miR-206 at the posttranscriptional level. Thus, lack of posttranscriptional downregulation may underlie Met overexpression in RMS and possibly in other types of cancer. Restoration of Met signalling in miR-206–expressing RMS cells via its constitutively active form (Tpr-Met) counteracted the effects of the miRNA, proving that sustained Met expression is one of the factors through which the lack of miR-1/miR-206 contributes to the pathogenesis of RMS.

In previous work, we have shown that Met silencing via RNAi reduces the oncogenicity of RMS cells in culture and in vivo, mainly by increasing apoptosis (29). Recently, 2 papers described the suppressive effect of ectopic expression of miR-1 in hepatocellular carcinoma and non–small cell lung cancer (NSCLC) cells, in which Met and miR-1 are also, respectively, overexpressed and underrepresented, relative to the corresponding nonneoplastic tissues (14, 37). In these works, growth inhibition, apoptosis, and loss of tumorigenic properties were entirely ascribed by the authors to the ability of miR-1 to silence the Met receptor. Met silencing may play a major role also in the inhibition of the malignant features of RMS by miR-1/miR-206. However, in our hands, the effects of the shRNA and of miR-1/miR-206 were not overlapping. In particular, Met silencing via RNAi was more efficient than miR-1/miR-206 in inducing apoptosis (29), while the miRNA was only mildly apoptotic but promoted myogenic differentiation. Thus, we conclude that in RMS the mere loss of Met leads to massive apoptosis, but, when occurring in the presence of a concomitant differentiative signal, it leads to differentiation.

Based on the ability of miR-1 and miR-206 to act as a differentiating agent in RMS cells in culture, we proceeded to test the therapeutic potential of miR-206 by inducing its expression in tumors derived from ERMS or ARMS cells transplanted into nude mice. Although there was no regression, the tumors stopped growing, and the vast majority of the cells exited from the cell cycle and underwent full myogenic differentiation. The results of this experiment constitute the first in vivo proof of concept that miR-206 may have therapeutic potential in RMS as a differentiative agent.

It should be noted, however, that while continuous doxycycline administration kept the tumor in check for the entire period of observation (over 3 months), in approximately 2 weeks after doxycycline withdrawal, the tumor resumed an aggressive modality of growth (data not shown). This suggests that a minor but relevant fraction of the RMS cells, in spite of the proliferative block, did not express a sufficient amount of miR-206 to achieve terminal differentiation. Thus, as in the case of retinoic acid and acute promyelocytic leukemia (APL), chronic administration of miR-206 would be necessary to ensure a permanent block of tumor growth.

Recent work has shown that transfection of the neural-enriched miR-124 induces morphological changes and expression of neuronal markers in mouse neural and brain tumor-derived stem cells as well as in human glioblastoma multiforme–derived (GBM-derived) stem cells (42). This and our findings suggest that other tissue-specific miRNAs could promote differentiation of related solid malignancies. miRNAs that participate in the control of chromatin remodelling may also hold such potential. For example miR-29, a ubiquitous miRNA previously shown to suppress tumorigenicity by normalizing aberrant patterns of methylation in NSCLC cells (43), has recently been proposed as an enhancer of myogenic differentiation and a suppressor of RMS (31).

Initially, RNAi-based therapeutics, in spite of the still largely unsolved problems of delivery, raised great expectations based on their ability to specifically target dominant oncogenes to which the cancer cells may be addicted. However, the recent discovery that individual cancers carry many more mutations than previously thought and that patients with the same diagnosis can harbor different sets of mutations (44–46) has cast serious doubts that such drugs will be active against most solid tumors. Strategies based on differentiative agents have so far been successfully applied only to hematological cancers, such as APL (47). Differentiation-based nontoxic treatments would be most desirable also for solid tumors, especially in the case of pediatric cancers (RMS or neuroblastomas) or of deadly brain tumors that are impossible to treat surgically or are resistant to traditional therapies (GBM). Our results were obtained in vivo, using cells of 2 RMS subtypes, harboring remarkably different genetic lesions (27), including nonfunctional mutations of p53 (48). Silber's results (42) were obtained in cell culture, using murine tumor-derived stem cells and also long-established human GBM cell lines. Based on these considerations, we propose that tissue-specific miRNAs may hold greater therapeutic potential than targeted drugs, since their differentiative power is based on the ability to influence the expression of thousands of genes and thus may not be compromised by a heterogenous genetic landscape.

## Methods

*Reagents*. All reagents, unless otherwise specified, were from Sigma-Aldrich.

*Cell culture, cell sorting, and primary samples*. RMS cells of embryonal (RD, RD18, HTB82, and TE671) and alveolar (RH4 and RH30) histotype and primary hMBs were grown in DMEM (Euroclone), supplemented with 10% FBS (Euroclone). All RMS cell lines were differentiated in DMEM with 5% horse serum (HS). hMBs were differentiated in DMEM plus 4.5 mg/ml glucose, 0.5% BSA, 10 ng/ml EGF, 0.15 mg/ml creatine, 5 ng/ml insulin, and 7 mM HEPES, pH 7.4. HTB82 and TE671 cells were a gift of Alessandra Pistilli (University of Perugia, Perugia, Italy), and hMBs were provided by Susan Treves (Basel University Hospital, Basel, Switzerland). Satellite cells were isolated from the hind-limb muscles of a 18-day-old *Ink4a*$^{-/-}$ mouse as previously described (49). Proliferating cells were kept in complete growth medium (F-10 HAM's nutrient mixture containing 20% FBS, 3% chicken embryo extract, and 2.5 ng/ml basic FGF [Peprotech]) on 0.5% gelatin-coated plates). To obtain differentiation into myotubes, cells were plated at subconfluence on gelatin-coated plates, kept in growth medium for 24 hours, and then switched to differentiation medium (DMEM containing 5% HS). All cells were incubated at 37°C in a 7% $CO_2$-water–saturated atmosphere, and media were supplemented with 2 mM L-glutamine, 100 U/ml penicillin, and 0.1 mg/ml streptomycin.

For cell sorting, cells were suspended at the concentration of $1 \times 10^7$/ml in basic sorting buffer (5 mM EDTA, 25 mM HEPES, pH 7.0, 1% heat-inactivated FBS) and then sorted for GFP expression on a MoFlo High-Performance Cell Sorter (Dako).

Primary human RMS specimens (or their RNA) of embryonal and alveolar histology and muscle tissues, provided by Samuel Singer (Memorial Sloan-Kettering Cancer Center), were procured at Memorial Sloan-Kettering Cancer Center and the Ospedale Infantile Regina Margherita. Human tissues were obtained following informed consent and with obscured identity according to the recommendations of the Institutional Review Board of the Memorial Sloan-Kettering Cancer Center and of the "Comitato Etico dell' Azienda Ospedaliera Ospedale Infantile Regina Margherita/S. Anna", both of which provided approval for these studies.

*Western blot*. Cells were washed with ice-cold PBS, lysed, and scraped in lysis buffer (20 mM Tris, pH 7.4, 150 mM NaCl, 5 mM EDTA, 1% Triton X-100) with 1 mM phenylmethylsulfonyl fluoride, 10 mM NaF, 1 mM $Na_3VO_4$, and protease inhibitor cocktail. Protein lysates were cleared of cellular debris by centrifugation at 4°C for 10 minutes at 12,000 *g*, quantified using Bio-Rad protein assay, resolved in 10% SDS-PAGE gels, and transferred to Hybond ECL Nitrocellulose Membranes (Amersham Biosciences). Proteins were visualized with horseradish peroxidase–conjugated secondary antibodies and SuperSignal West Pico Chemiluminescent Substrate (Pierce).

*Antibodies*. Anti-Met was from Zymed; anti–cyclin D1, anti-p21, and anti-myogenin were from Santa Cruz Biotechnology Inc.; anti–α-tubulin (B-5-1-1) was from Sigma-Aldrich; anti-GFP was from Molecular Probes; anti-MHC was from Developmental Studies Hybridoma Bank; anti–phospho-pRb and anti–phospho-p38 were from Cell Signaling Technology; and anti-Ki67 was from Novocastra.

*Real-time PCR and Northern blot*. RNA was extracted using TRIzol (Invitrogen) for cells and snap-frozen tissues and MasterPure RNA Purification Kit (Epicentre Biotechnologies) for formalin-fixed, paraffin-embedded tissues. TaqMan miRNA Assays (Applied Biosystems) were used for absolute and relative quantification of mature miR-1 and miR-206 expression levels. miR-16 was used to normalize the results. Reverse transcription and real-time PCR were performed according to the manufacturer's instructions. To determine absolute expression of miRNAs, a standard curve was generated using a purified RNA oligonucleotide corresponding to miR-206 (Sigma-Aldrich) at the known concentrations of $10^{-3}$, $10^{-2}$, $10^{-1}$, $10^0$, $10^1$, and $10^2$ femtomoles. One hundred nanograms of total RNA were analyzed using the TaqMan miRNA Assay. TaqMan Ct values for each sample reaction were then converted into absolute values (femtomoles) based on the standard curve. For quantitative Northern blot analysis of miRNAs, 5 μg of total RNA were electrophoresed in a 15% polyacrylamide-urea gel and transferred by electroblotting onto Hybond-$N^+$ membrane (Amersham Biosciences). Hybridization was performed with the following $^{32}$P-labeled DNA oligos: anti–miR-1, 5′-ATACATACTTCTTTACATTCCA-3′; anti–miR-206, 5′-CCACACACTTCCTTACATTCCA-3′; anti-U6, 5′-TGTGCTGCCGAAGCGAGCAC-3′. Synthetic mature miRNAs used as standards were purchased from Sigma-Aldrich.

For Met detection, 1 μg of total RNA was used for reverse transcription with iScript cDNA Synthesis Kit (Bio-Rad) according to the manufacturer's protocol. Real-time PCR was performed with iQ SYBR Green (Bio-Rad) with the

following primers: Met forward 5′-CGCTACGATGCAAGAGTACACA-3′, Met reverse 5′-TTAGGAAACTGATCTTCTGGA-3′, HPRT forward 5′-TGACACTGGCAAAACAATGCA-3′, and HPRT reverse 5′-GGTCCTTTTCACCAGCAAGCT-3′ as an internal control. Real-time PCR parameters were as follows: cycle 1, 95°C for 3 minutes; cycle 2, 95°C for 15 seconds, 60°C 30 seconds for 40 cycles. The 2-ΔΔCT method was used to analyze the data.

*Vector production, viral transduction, and LNA transfection*. NaldimiR-206 lentiviral vector was generated by PCR amplification of the pre–miR-206 locus from human genomic DNA with the following primers: pre–miR-206 forward, 5′-GTCCGCGGGGCAAGGAGGAAAGATGCTA-3′ and pre–miR-206 reverse, 5′-CTGGTACCCTGGGGCCAGCGAGGAGGC-3′. The PCR product was sequenced and then cloned into the SacII and KpnI sites of pCCL.sin.PPT.hPGK.GFPWpre vector provided by Luigi Naldini (San Raffaele-Telethon Institute for Gene Therapy, Milano, Italy) (50). An analogous procedure was used for NaldimiR-206AS preparation but with the following primers: pre–miR-206AS forward 5′-GTCCGCGGCTGGGGCCAGCGAGGAGGC-3′ and pre–miR-206AS reverse 5′-CTGGTACCGGCAAGGAGGAAAGATGCTA-3′. Conditional NpBI-206 and NpBI-206AS lentiviral vectors were generated by subcloning the bidirectional tetracycline-responsive element–GFP cassette from pBI vector (Clontech) into NaldimiR-206 and NaldimiR-206AS, respectively, between the EcoRV and SalI sites. Concentrated lentiviral vector stocks were produced as previously described (29). To obtain regulatable expression of miR-206, cells were transduced first with a lentiviral vector expressing the tetracycline transactivator (tTA) (for Tet-off system) or reverse tTA (rtTA) (Tet-on system) transactivator and subsequently with the responder vector NpBI-206 or NpBI-206AS. The transactivators bind to the minimal CMV promoter in absence (Tet-off) or presence (Tet-on) of doxycycline. The Tet-off inducible system enabled us to select high–miR-206 expressers by sorting cells grown without doxycycline based on their green fluorescence. The sorted cells were then allowed to recover with doxycycline. Successive doxycycline withdrawal resulted in expression of miR-206. The Tpr-Met retrovirus, provided by Francesco Boccalatte (CeRMS, University of Torino), was generated by subcloning the Tpr-Met cDNA into blunted EcoRI and BamHI sites of the Pallino retroviral vector (51).

Human Met 3′UTR was PCR amplified from genomic DNA using the following primers, forward 5′-TGCCGCGGATGATGAGGTGGACACACGA-3′, reverse 5′-CTCCGCGGCGAAGTACCATTCAGTTCAGC-3′, and cloned downstream of GFP in the SacII restriction site of the pCCL.sin.PPT.hPGK.GFPWpre lentiviral vector (50) that was then sequenced and used for cotransfection experiments. We constructed the 4X miR-1/miR-206 sensor vector by annealing the following oligonucleotides: forward 1, 5′-GGTATAAATTTTTGTATAGACATTCCTCGATTATAAATTTTTGTATAGACATTCCTA-3′, forward 2, 5′-AGCTTTCACCCATTAGGTAAACATTCCCCGATTCACCCATTAGGTAAACATTCCCGGTAC-3′, reverse 1, 5′-CGGGAATGTTTACCTAATGGGTGAATCGGGGAATGTTTACCTAATGGGTGAA-3′, reverse 2, 5′- AGCTTAGGAATGTCTATACAAAAATTTATAATCGAGGAATGTCTATACAAAAATTTATACCGC-3′. The resulting vector contained 2 copies of both miR-1/miR-206–binding sites predicted by Targetscan in Met 3′UTR. We then subcloned the annealed oligonucleotides into the SacII/KpnI sites of the aforementioned lentiviral vector. The same procedure was followed to generate the 4X point-mutated sensor vector using the following primers: forward 1, 5′- GGTATAACTTTTTGGATAGCACGGAATCGATTATAACTTTTTGGATAGCACGGAATA-3′; forward 2, 5′-AGCTTTAACACATTAGGTAACACGGAACCGATTAACACATTAGGTAACACGGAACGGTAC-3′; reverse 1, 5′-CGTTCCGTGTTACCTAATGTGTTAATCGGTTCCGTGTTACCTAATGTGTTAA-3′; reverse 2, 5′-AGCTTATTCCGTGCTATCCAAAAAGTTATAATCGATTCCGTGCTATCCAAAAAGTTATACCGC-3′. Predesigned miRCURY LNA probes were purchased from Exiqon. All transfection were performed with Lipofectamine 2000 (Invitrogen) according to the manufacturer's instructions.

*Cell proliferation assay*. Cells were seeded in 96-well plates at a density of $2 \times 10^3$ cells/well. Proliferation was evaluated by MTT labeling reagent (Roche).

*Anchorage-independent cell-growth assay*. Cells were suspended in 0.35% type VII low-melting agarose in 10% DMEM at $2 \times 10^4$ per well and plated on a layer of 0.7% agarose in 10% DMEM in 6-well plates and cultured at 37°C with 7% $CO_2$. After 2 weeks, colonies of more than 100 μm in diameter were counted.

*Immunofluorescence*. For MHC detection, cells seeded on 24-well plates and either treated or not with 1 μg/ml doxycycline for 6 days in medium with high levels of serum were fixed for 20 minutes with ice-cold methanol/acetone 2:1, washed in PBS, and saturated in blocking solution (3% BSA in PBS) for 1 hour. Once permeabilized with 0.3% Triton X-100 for 5 minutes, cells were incubated with MHC primary antibody for 1 hour and then with Cy3-conjugated anti-mouse antibody (1:200) for 30 minutes. Nuclei were then stained with DAPI. MHC- and DAPI-positive cells were counted with ImageJ (http://rsbweb.nih.gov/ij/) at ×20 magnification (6 fields per well).

*Cell-cycle analysis*. Cells were plated at a density of $1 \times 10^5$ in 6-well plates and then treated or not with doxycycline (1 μg/ml) for 3 days. After being harvested and washed with PBS, $5 \times 10^5$ cells were treated with RNAse (0.25 mg/ml) and stained with propidium iodide (50 μg/ml). The cell-cycle distribution in $G_0/G_1$, S, and $G_2/M$ phase was calculated using the CellQuest program (BD Biosciences).

*Assessment of apoptosis*. Apoptosis was measured by flow cytometry after staining with Annexin V. Briefly, after 5 days with or without doxycycline (1 μg /ml), cells ($1 \times 10^5$) were trypsinized, washed in PBS, and incubated for 15 minutes at 37°C in HEPES buffer solution (10 mM HEPES, pH 7.4, 140 mM NaCl, 2.5 mM $CaCl_2$) with 2.5 μl biotin-conjugated Annexin V (BD Biosciences). Annexin V binding was revealed by additional incubation with 0.5 μl streptavidin-allophycocyanin (APC; BD Biosciences). Cells were analyzed by FACScan using CellQuest Software (BD Biosciences).

*In vitro invasion assay*. Invasiveness was examined by using the membrane invasion culture system (Transwell Polycarbonate Membranes; 6.5-mm diameter, 8-μm pore size; Corning Life Sciences) according to the standard protocol. Briefly, $2 \times 10^5$ cells were seeded, in presence or absence of doxycycline (1 μg/ml), onto the upper well of transwells previously coated with 50 μl of Matrigel Basement Membrane Matrix (BD Biosciences). After 72 hours, the noninvasive cells on the upper surface of the membrane were removed with a cotton swab. Cells that migrated through the Matrigel matrix and attached to the lower surface of the membrane were fixed with 11% glutaraldehyde, stained with cresyl violet, solubilized in 10% acetic acid solution, and quantified by spectrophotometrical analysis (595 nm).

*Microarrays and data analysis*. Affymetrix Human GeneChip Gene ST 1.0 arrays (Affymetrix) were hybridized at the Cogentech core facility (Institute of Molecular Oncology Foundation–European Institute of Oncology Campus, Milano, Italy) according to standard Affymetrix protocols. One microgram of total RNA was used as starting material for each sample. The experiment included 3 independent skeletal muscles ($n = 3$) and 6 biological replicates of RD18 cells previously infected with the inducible NpBI-206 vector and then treated or not with doxycycline (Tet-on), thus giving rise to both miR-206–induced ($n = 4$) and miR-206–noninduced ($n = 2$) cells. Moreover, NpBI-206AS–infected cells were used as additional controls in both induced and noninduced conditions. The array data were analyzed with the Partek Genomics Suite version 6.3 software (Partek Inc.). All 734 genes showing differential expression between the 2 experimental conditions in RD18 cells found to be significant by ANOVA (fold change compared to the mean across the whole panel was greater than 2 and the Student's *t* test *P* value was lower than 0.05) were then subjected to unsupervised, hierarchical clustering. Normal muscle samples were also included in the clustering. The same set of up- and downregulated genes was

further analyzed to reveal enrichment of functional categories using the Database for Annotation, Visualization and Integrated Discovery (DAVID) 2008 (http://david.abcc.ncifcrf.gov/). We used the Functional Annotation Tool program and reported only GOTERM-BPs (Gene Ontology Terms that identify genes involved in a particular Biological Process) that had *P* values of less than 0.05 after correcting for multiple testing. The EIMMo miRNA target prediction server (http://www.mirz.unibas.ch/ElMMo2/) was used to identify putative miR-206 targets among the downregulated transcripts in miR-206–induced compared to noninduced RD18 cells.

*In vivo tumorigenesis assay*. All animal procedures were approved by the Ethical Committee of the University of Torino and by the Italian Ministry of Health. Cells were trypsinized and resuspended at $1 \times 10^7$ cells/ml in sterile PBS. Cells (200 μl) were injected subcutaneously into the flank of female *nu/nu* mice (Charles River Laboratories). Tumor size was measured with Vernier calipers every 3 days, and tumor volumes were calculated as the volume of a sphere. Conditional miR-206 expression was induced in mice by adding (Tet-on system) or not (Tet-off system) 1 mg/ml of doxycycline in the drinking water. It has to be noted that with the Tet-off system we observed a 2-week lag time after induction before GFP expression. Furthermore, fluorescence was rather weak and spotty in the tumors. On the contrary, GFP was detectable after just 48 hours of induction with the Tet-on system, which was therefore chosen for the experiments in which miR-206 was induced in already palpable tumors.

*Immunohistochemistry*. Tumor samples were collected at the indicated times, fixed for 2 hours in 4% paraformaldehyde, and embedded in paraffin. Rehydrated sections were treated with 3% $H_2O_2$ and microwaved for 30 minutes in 10 mM Antigen Retrieval Citra (Biogenex). All antibody incubations were performed at room temperature with the solutions provided by the Dako LSAB2 System-HRP kit (primary antibody, 1 hour; peroxidase-conjugated secondary antibody, 30 minutes). Staining was developed by liquid diaminobenzidine chromogen (Biogenex) followed by hematoxylin.

*Statistics*. For experiments in which 2 variables were compared, 2-tailed unpaired Student's *t* tests were used. Three-way ANOVA was performed to analyze the microarray data. For functional annotation using DAVID, significance was calculated following Benjamini-Hochberg False Discovery Rate multiple testing correction. *P* values of less than 0.05 were considered statistically significant.

## Acknowledgments

We are particularly grateful to Giorgio Inghirami, Roberto Chiarle, and Bob Milne for critically revising the manuscript and to all members of our laboratories for helpful discussions and comments. We thank Paolo Accornero, Silvia Miretti, Sharon Mazzero, Simona Perga, and Michela Nalin for technical help. We also thank Simone Minardi, Jean Hausser, and Hanah Margalit for their critical support with the microarray data analysis. We are grateful to Susan Treves for the primary hMBs, to Samuel Singer for providing normal muscle samples used in this work, and to Luigi Naldini for the lentiviral vectors. This work was supported by funding from the Italian Association for Cancer Research, the Oncology Project Compagnia di San Paolo/FIRMS (CeRMS), the APIN project 2005–2006 of the Rotaract District 2030, the Regione Piemonte-Ricerca Sanitaria Finalizzata, and the Sixth Research Framework Programme of the European Union, Project RIGHT (LSHB-CT-2004-005276).

Received for publication November 17, 2008, and accepted in revised form May 27, 2009.

Address correspondence to: Carola Ponzetto, Department of Anatomy, Pharmacology and Forensic Medicine, University of Torino, C.so Massimo d'Azeglio 52, 10126 Torino, Italy. Phone: 39-011-6707799; Fax: 39-011-6705931; E-mail: carola.ponzetto@unito.it.

1. Stefani, G., and Slack, F.J. 2008. Small non-coding RNAs in animal development. *Nat. Rev. Mol. Cell Biol.* **9**:219–230.
2. Bartel, D.P. 2004. MicroRNAs: genomics, biogenesis, mechanism, and function. *Cell.* **116**:281–297.
3. Lee, R.C., and Ambros, V. 2001. An extensive class of small RNAs in Caenorhabditis elegans. *Science.* **294**:862–864.
4. Lim, L.P., et al. 2005. Microarray analysis shows that some microRNAs downregulate large numbers of target mRNAs. *Nature.* **433**:769–773.
5. Baek, D., et al. 2008. The impact of microRNAs on protein output. *Nature.* **455**:64–71.
6. Selbach, M., et al. 2008. Widespread changes in protein synthesis induced by microRNAs. *Nature.* **455**:58–63.
7. Calin, G.A., et al. 2004. Human microRNA genes are frequently located at fragile sites and genomic regions involved in cancers. *Proc. Natl. Acad. Sci. U. S. A.* **101**:2999–3004.
8. Garzon, R., Fabbri, M., Cimmino, A., Calin, G.A., and Croce, C.M. 2006. MicroRNA expression and function in cancer. *Trends Mol. Med.* **12**:580–587.
9. Lu, J., et al. 2005. MicroRNA expression profiles classify human cancers. *Nature.* **435**:834–838.
10. Kumar, M.S., Lu, J., Mercer, K.L., Golub, T.R., and Jacks, T. 2007. Impaired microRNA processing enhances cellular transformation and tumorigenesis. *Nat. Genet.* **39**:673–677.
11. Yu, F., et al. 2007. let-7 regulates self renewal and tumorigenicity of breast cancer cells. *Cell.* **131**:1109–1123.
12. Kumar, M.S., et al. 2008. Suppression of non-small cell lung tumor development by the let-7 microRNA family. *Proc. Natl. Acad. Sci. U. S. A.* **105**:3903–3908.
13. He, L., et al. 2007. A microRNA component of the p53 tumour suppressor network. *Nature.* **447**:1130–1134.
14. Nasser, M.W., et al. 2008. Downregulation of microRNA-1 (miR-1) in lung cancer: Suppression of tumorigenic property of lung cancer cells and their sensitization to doxorubicin induced apoptosis by miR-1. *J. Biol. Chem.* **283**:33394–33405.
15. Lagos-Quintana, M., et al. 2002. Identification of tissue-specific microRNAs from mouse. *Curr. Biol.* **12**:735–739.
16. Babak, T., Zhang, W., Morris, Q., Blencowe, B.J., and Hughes, T.R. 2004. Probing microRNAs with microarrays: tissue specificity and functional inference. *RNA.* **10**:1813–1819.
17. Baskerville, S., and Bartel, D.P. 2005. Microarray profiling of microRNAs reveals frequent coexpression with neighboring miRNAs and host genes. *RNA.* **11**:241–247.
18. Wienholds, E., et al. 2005. MicroRNA expression in zebrafish embryonic development. *Science.* **309**:310–311.
19. McCarthy, J.J. 2008. MicroRNA-206: The skeletal muscle-specific myomiR. *Biochim. Biophys. Acta.* **1779**:682–691.
20. Takada, S., et al. 2006. Mouse microRNA profiles determined with a new and sensitive cloning method. *Nucleic Acids Res.* **34**:e115.
21. Anderson, C., Catoe, H., and Werner, R. 2006. MIR-206 regulates connexin43 expression during skeletal muscle development. *Nucleic Acids Res.* **34**:5863–5871.
22. Chen, J.F., et al. 2006. The role of microRNA-1 and microRNA-133 in skeletal muscle proliferation and differentiation. *Nat. Genet.* **38**:228–233.
23. Kim, H.K., Lee, Y.S., Sivaprasad, U., Malhotra, A., and Dutta, A. 2006. Muscle-specific microRNA miR-206 promotes muscle differentiation. *J. Cell. Biol.* **174**:677–687.
24. Wachtel, M., et al. 2006. Subtype and prognostic classification of rhabdomyosarcoma by immunohistochemistry. *J. Clin. Oncol.* **24**:816–822.
25. Shapiro, D.N., Sublett, J.E., Li, B., Downing, J.R., and Naeve, C.W. 1993. Fusion of PAX3 to a member of the forkhead family of transcription factors in human alveolar rhabdomyosarcoma. *Cancer Res.* **53**:5108–5112.
26. Davis, R.J., D'Cruz, C.M., Lovell, M.A., Biegel, J.A., and Barr, F.G. 1994. Fusion of PAX7 to FKHR by the variant t(1;13)(p36;q14) translocation in alveolar rhabdomyosarcoma. *Cancer Res.* **54**:2869–2872.
27. Laé, M., et al. 2007. Global gene expression profiling of PAX-FKHR fusion-positive alveolar and PAX-FKHR fusion-negative embryonal rhabdomyosarcomas. *J. Pathol.* **212**:143–151.
28. Sharp, R., et al. 2002. Synergism between INK4a/ARF inactivation and aberrant HGF/SF signaling in rhabdomyosarcomagenesis. *Nat. Med.* **8**:1276–1280.
29. Taulli, R., et al. 2006. Validation of met as a therapeutic target in alveolar and embryonal rhabdomyosarcoma. *Cancer Res.* **66**:4742–4749.
30. Subramanian, S., et al. 2008. MicroRNA expression signature of human sarcomas. *Oncogene.* **27**:2015–2026.
31. Wang, H., et al. 2008. NF-kappaB-YY1-miR-29 regulatory circuitry in skeletal myogenesis and rhabdomyosarcoma. *Cancer Cell.* **14**:369–381.
32. Astolfi, A., et al. 2001. Identification of new genes related to the myogenic differentiation arrest of human

rhabdomyosarcoma cells. *Gene.* **274**:139–149.
33. Anastasi, S., et al. 1997. A natural hepatocyte growth factor/scatter factor autocrine loop in myoblast cells and the effect of the constitutive Met kinase activation on myogenic differentiation. *J. Cell Biol.* **137**:1057–1068.
34. Park, M., et al. 1986. Mechanism of met oncogene activation. *Cell.* **45**:895–904.
35. McCarthy, J.J., and Esser, K.A. 2007. MicroRNA-1 and microRNA-133a expression are decreased during skeletal muscle hypertrophy. *J. Appl. Physiol.* **102**:306–313.
36. Rao, P.K., Kumar, R.M., Farkhondeh, M., Baskerville, S., and Lodish, H.F. 2006. Myogenic factors that regulate expression of muscle-specific microRNAs. *Proc. Natl. Acad. Sci. U. S. A.* **103**:8721–8726.
37. Datta, J., et al. 2008. Methylation mediated silencing of MicroRNA-1 gene and its role in hepatocellular carcinogenesis. *Cancer Res.* **68**:5049–5058.
38. Tapscott, S.J., Thayer, M.J., and Weintraub, H. 1993. Deficiency in rhabdomyosarcomas of a factor required for MyoD activity and myogenesis. *Science.* **259**:1450–1453.
39. Lluís, F., Perdiguero, E., Nebreda, A.R., and Muñoz-Cánoves, P. 2006. Regulation of skeletal muscle gene expression by p38 MAP kinases. *Trends Cell. Biol.* **16**:36–44.
40. Puri, P.L., et al. 2000. Induction of terminal differentiation by constitutive activation of p38 MAP kinase in human rhabdomyosarcoma cells. *Genes Dev.* **14**:574–584.
41. Boutz, P.L., Chawla, G., Stoilov, P., and Black, D.L. 2007. MicroRNAs regulate the expression of the alternative splicing factor nPTB during muscle development. *Genes Dev.* **21**:71–84.
42. Silber, J., et al. 2008. miR-124 and miR-137 inhibit proliferation of glioblastoma multiforme cells and induce differentiation of brain tumor stem cells. *BMC Med.* **6**:14.
43. Fabbri, M., et al. 2007. MicroRNA-29 family reverts aberrant methylation in lung cancer by targeting DNA methyltransferases 3A and 3B. *Proc. Natl. Acad. Sci. U. S. A.* **104**:15805–15810.
44. Parsons, D.W., et al. 2008. An integrated genomic analysis of human glioblastoma multiforme. *Science.* **321**:1807–1812.
45. Jones, S., et al. 2008. Core signaling pathways in human pancreatic cancers revealed by global genomic analyses. *Science.* **321**:1801–1806.
46. The Cancer Genome Atlas Research Network. 2008. Comprehensive genomic characterization defines human glioblastoma genes and core pathways. *Nature.* **455**:1061–1068.
47. Ohno, R., et al. 1993. Multi-institutional study of all-trans-retinoic acid as a differentiation therapy of refractory acute promyelocytic leukemia. Leukaemia Study Group of the Ministry of Health and Welfare. *Leukemia.* **7**:1722–1727.
48. Ganjavi, H., Gee, M., Narendran, A., Freedman, M.H., and Malkin, D. 2005. Adenovirus-mediated p53 gene therapy in pediatric soft-tissue sarcoma cell lines: sensitization to cisplatin and doxorubicin. *Cancer Gene Ther.* **12**:397–406.
49. Crepaldi, T., et al. 2007. Conditional activation of MET in differentiated skeletal muscle induces atrophy. *J. Biol. Chem.* **282**:6812–6822.
50. Follenzi, A., Ailles, L.E., Bakovic, S., Geuna, M., and Naldini, L. 2000. Gene transfer by lentiviral vectors is limited by nuclear translocation and rescued by HIV-1 pol sequences. *Nat. Genet.* **25**:217–222.
51. Grignani, F., et al. 1998. High-efficiency gene transfer and selection of human haematopoietic progenitor cells with a hybrid EBV/retroviral vector expressing the green fluorescence protein. *Cancer Res.* **58**:14–19.